



Detection of Adsorbed Water and Hydroxyl on the Moon

Roger N. Clark
Science **326**, 562 (2009);
DOI: 10.1126/science.1178105

This copy is for your personal, non-commercial use only.

If you wish to distribute this article to others, you can order high-quality copies for your colleagues, clients, or customers by [clicking here](#).

Permission to republish or repurpose articles or portions of articles can be obtained by following the guidelines [here](#).

The following resources related to this article are available online at www.sciencemag.org (this information is current as of November 7, 2013):

Updated information and services, including high-resolution figures, can be found in the online version of this article at:

<http://www.sciencemag.org/content/326/5952/562.full.html>

Supporting Online Material can be found at:

<http://www.sciencemag.org/content/suppl/2009/09/24/1178105.DC1.html>

A list of selected additional articles on the Science Web sites **related to this article** can be found at:

<http://www.sciencemag.org/content/326/5952/562.full.html#related>

This article **cites 16 articles**, 1 of which can be accessed free:

<http://www.sciencemag.org/content/326/5952/562.full.html#ref-list-1>

This article has been **cited by** 8 article(s) on the ISI Web of Science

This article has been **cited by** 4 articles hosted by HighWire Press; see:

<http://www.sciencemag.org/content/326/5952/562.full.html#related-urls>

This article appears in the following **subject collections**:

Planetary Science

http://www.sciencemag.org/cgi/collection/planet_sci

mation to afford the ligand-centered radical intermediate **6'** (Fig. 4). In the case of the smaller NHC **2**, because of a lack of kinetic protection as well as strong binding of the carbene ligand, the dimerization process of **6** proceeds and the mixed valent Fe(0)–Fe(I) species is formed stoichiometrically (Fig. 2). However, when the more sterically demanding NHC **7** interacts with the iron center, the dimerization process is blocked, and the unstable species **6'** extrudes the NHC ligand. The ensuing Fe₂(COT)₂ species rapidly combines with Fe(COT)₂ to form the tri-iron cluster. Of course, it is possible that the NHC may not dissociate until the third Fe(COT) fragment is added to **6'**. There is ample precedent in the literature for NHC lability, particularly in zero-valent, late transition-metal complexes (38). Moreover, steric hindrance at the metal center reportedly facilitates this process (39).

Once thought of only as laboratory curiosities, stable carbenes are now widely recognized as indispensable tools for organic synthesis. The NHC-mediated reactions we explored provide a foundation on which to develop future organometallic transformations catalyzed by NHCs, as well as other small organic species.

References and Notes

- R. A. Moss, M. S. Platz, M. Jones Jr., Eds., *Reactive Intermediate Chemistry* (Wiley, New York, 2004).
- A. Igau, H. Grutzmacher, A. Baceirodo, G. Bertrand, *J. Am. Chem. Soc.* **110**, 6463 (1988).
- A. J. Arduengo, R. L. Harlow, M. Kline, *J. Am. Chem. Soc.* **113**, 361 (1991).

- F. E. Hahn, M. C. Jahnke, *Angew. Chem. Int. Ed.* **47**, 3122 (2008).
- R. H. Crabtree, *Coord. Chem. Rev.* **251**, 595 (2007).
- J. Vignolle, X. Catton, D. Bourissou, *Chem. Rev.* **109**, 3333 (2009).
- O. Schuster, L. Yang, H. G. Raubenheimer, M. Albrecht, *Chem. Rev.* **109**, 3445 (2009).
- M. Alcarazo, C. W. Lehmann, A. Anoop, W. Thiel, A. Fürstner, *Nat. Chem.* **1**, 295 (2009).
- O. Kauffhold, F. E. Hahn, *Angew. Chem. Int. Ed.* **47**, 4057 (2008).
- V. Lavallo, Y. Canac, B. Donnadieu, W. W. Schoeller, G. Bertrand, *Angew. Chem. Int. Ed.* **45**, 3488 (2006).
- J. D. Masuda, W. W. Schoeller, B. Donnadieu, G. Bertrand, *Angew. Chem. Int. Ed.* **46**, 7052 (2007).
- G. D. Frey, V. Lavallo, B. Donnadieu, W. W. Schoeller, G. Bertrand, *Science* **316**, 439 (2007).
- Y. Z. Wang *et al.*, *Science* **321**, 1069 (2008).
- D. Enders, A. A. Narine, *J. Org. Chem.* **73**, 7857 (2008).
- R. H. Grubbs, *Angew. Chem. Int. Ed.* **45**, 3760 (2006).
- C. Samojłowicz, M. Bieniek, K. Grela, *Chem. Rev.* **109**, 3708 (2009).
- R. Breslow, E. Mcnelis, *J. Am. Chem. Soc.* **81**, 3080 (1959).
- D. Enders *et al.*, *Angew. Chem. Int. Ed. Engl.* **34**, 1021 (1995).
- N. Marion, S. Diez-Gonzalez, S. P. Nolan, *Angew. Chem. Int. Ed.* **46**, 2988 (2007).
- D. A. Culkin *et al.*, *Angew. Chem. Int. Ed.* **46**, 2627 (2007).
- I. Resa, E. Carmona, E. Gutierrez-Puebla, A. Monge, *Science* **305**, 1136 (2004).
- T. Nguyen *et al.*, *Science* **310**, 844 (2005).
- S. P. Green, C. Jones, A. Stasch, *Science* **318**, 1754 (2007).
- P. J. Dyson, J. S. McIndoe, *Transition Metal Carbonyl Cluster Chemistry* (Gordon & Breach, Amsterdam, 2000).
- C. Bolm, J. Legros, J. Le Paih, L. Zani, *Chem. Rev.* **104**, 6217 (2004).
- B. D. Sherry, A. Fürstner, *Acc. Chem. Res.* **41**, 1500 (2008).
- A. Fürstner, *Angew. Chem. Int. Ed.* **48**, 1364 (2009).
- R. Mackenzi, P. L. Timms, *J. Chem. Soc. Chem. Commun.* 650 (1974).
- P. Le Floch *et al.*, *Eur. J. Inorg. Chem.* **1998** (1998).
- D. H. Gerlach, R. A. Schunn, *Inorg. Syn.* **15**, 2 (1974).
- H. Felkin, P. W. Lednor, J. M. Normant, R. A. J. Smith, *J. Organomet. Chem.* **157**, C64 (1978).
- Materials and methods are detailed in supporting material available on Science Online.
- M. Y. Darensbourg, E. J. Lyon, X. Zhao, I. P. Georgakaki, *Proc. Natl. Acad. Sci. U.S.A.* **100**, 3683 (2003).
- J. W. Peters, W. N. Lanzilotta, B. J. Lemon, L. C. Seefeldt, *Science* **282**, 1853 (1998).
- C. R. Hess, T. Weyhermuller, E. Bill, K. Wieghardt, *Angew. Chem. Int. Ed.* **48**, 3703 (2009).
- R. Desiderato, G. R. Dobson, *J. Chem. Educ.* **59**, 752 (1982).
- A. Carbonaro, A. Greco, G. Dallasta, *J. Organomet. Chem.* **20**, 177 (1969).
- N. D. Clement, K. J. Cavell, L. L. Ooi, *Organometallics* **25**, 4155 (2006).
- R. Dorta *et al.*, *J. Am. Chem. Soc.* **127**, 2485 (2005).
- We gratefully acknowledge financial support from NIH for grant 5R01 GM31332 and a National Research Service Award Postdoctoral Fellowship (to V.L.). We thank L. M. Henling and M. W. Day (California Institute of Technology) for x-ray crystallographic analysis. The Bruker KAPPA APEX II x-ray diffractometer was purchased via an NSF Chemistry Research Instrumentation and Facilities: Multi-User award to the California Institute of Technology, CHE-0639094. Crystallographic data for complexes **3** and **8** are available free of charge from the Cambridge Crystallographic Data Center under reference numbers CCDC-724011 and CCDC-728138, respectively.

Supporting Online Material

www.sciencemag.org/cgi/content/full/326/5952/559/DC1
Materials and Methods
References

10 July 2009; accepted 13 August 2009
10.1126/science.1178919

Detection of Adsorbed Water and Hydroxyl on the Moon

Roger N. Clark

Data from the Visual and Infrared Mapping Spectrometer (VIMS) on Cassini during its flyby of the Moon in 1999 show a broad absorption at 3 micrometers due to adsorbed water and near 2.8 micrometers attributed to hydroxyl in the sunlit surface on the Moon. The amounts of water indicated in the spectra depend on the type of mixing and the grain sizes in the rocks and soils but could be 10 to 1000 parts per million and locally higher. Water in the polar regions may be water that has migrated to the colder environments there. Trace hydroxyl is observed in the anorthositic highlands at lower latitudes.

The quest to find water on the Moon has been underway since the prediction of ice in the permanently shadowed craters in the polar regions (1, 2). Water is a vital resource needed by a human colony and played a fundamental role in planetary evolution (3). Spectroscopy is a tool that can be used to detect water and hydroxyl in the optical surface (the top few mm) using OH and H₂O absorptions near 1.5, 2, and 3 μm.

It is thought that the Moon formed by a collision between Earth and a Mars-sized body (4) about 4.4 × 10⁹ years ago. The impact and the

accretion of the debris heated the early Moon, creating an extensive lunar magma ocean (5, 6). These events are thought to have resulted in the loss of almost all volatiles in the Moon, and indeed evidence from Apollo and Luna samples indicate that lunar materials are deficient in volatiles compared with Earth (3). However, 20 to 45 parts per million (ppm) water occurs in some Apollo lunar glasses (7).

In addition, neutron spectrometer data from Lunar Prospector (LP) (8–10) showed that hydrogen is present in the lunar polar regions. I used data from the Visual and Infrared Mapping Spectrometer (VIMS) (11) on Cassini, which flew by the Moon on 19 August 1999, to map the dis-

tribution of water (Fig. 1). VIMS obtained 11 full and 2 partial image cubes with a spatial resolution of about 175 km per pixel and spectral coverage over the 0.35 to 5 μm with some gaps due to sensor saturation [supporting online material (SOM) text and fig. S1].

Where the moon is warmed by solar radiation, thermal emission contributes to the observed signal, $(I + T)/F$, where I is measured radiance plus thermal emission T and πF equals solar radiance. The thermal emission component and emissivity effects can mask weak water absorptions, but not strong ones, nor sharper absorptions due to hydroxyl. Thermal emission was computed and removed from lunar spectra (Fig. 2A) by using a thermal model (12, 13) (SOM text and figs. S2 and S3), which included estimating the emissivity from reflectance by using Kirchoff's law. Thermal-removed lunar spectra show water and hydroxyl absorptions in many but not all locations on the lunar disk (Figs. 1, E and F, and 2, A and B). The linear, positive-sloping spectral shape (Fig. 2A) is characteristic of the spectral signature of nanophase iron (14).

The lunar absorptions near 3 μm are characteristic of an O-H stretch fundamental in the H₂O molecule commonly seen in spectra of materials with adsorbed water or hydroxyl-bearing materials (Fig. 2, C and D) (15). The VIMS broad 3-μm absorption was strongest in the south lunar

U.S. Geological Survey, Mail Stop 964, Box 25046 Federal Center, Denver, CO 80227, USA. E-mail: rclark@usgs.gov

Fig. 1. Cassini VIMS observations of the Moon on 19 August 1999. The VIMS flyby view was south of the lunar equator. (A) VIMS 2.4- μm apparent reflectance. (B) Cassini Imaging Science Subsystem image obtained during the flyby. The yellow bars indicated the equator position. The yellow cross indicates latitude 0, longitude 0. (C) Locations of VIMS spectra in Fig. 2A in the 2.4- μm apparent reflectance image. (D) VIMS-derived temperatures. Maps of (E) 3- μm absorption strength (blue) and (F) 2.8- μm OH strength (orange and green). (G) Hydrogen map from LP (7–9) masked to give a similar view as the VIMS observation.

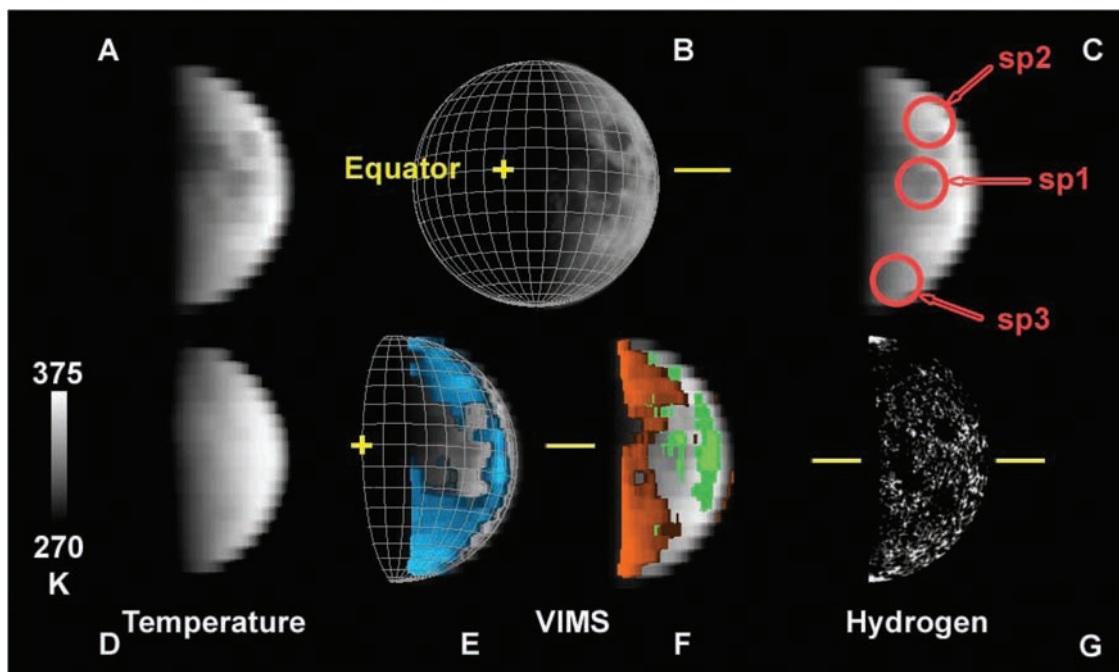
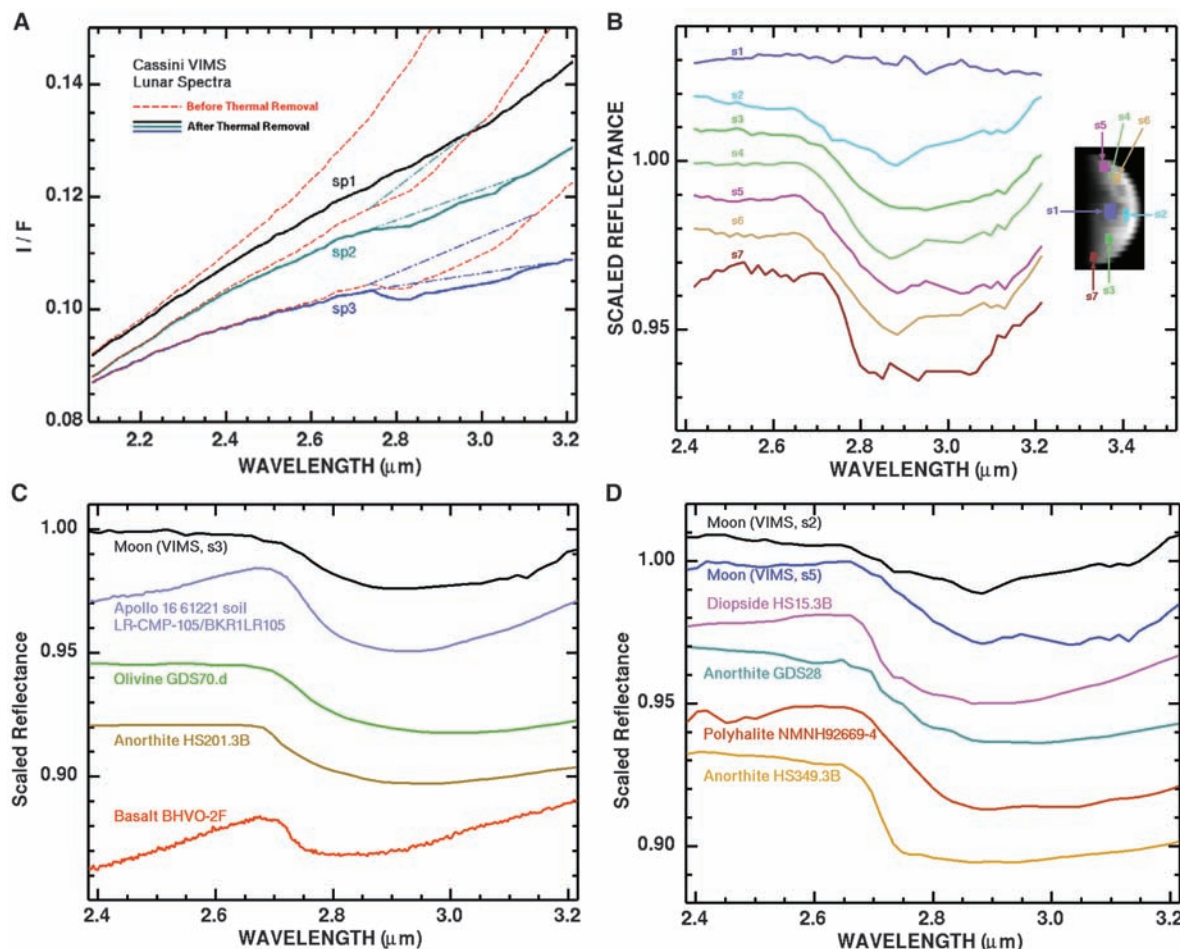


Fig. 2. (A) Average VIMS spectra for the three regions indicated in Fig. 1C. The spectra before thermal emission are shown as dashed red lines. Spectrum sp1 is dominated by maria and shows no water absorption. Spectrum sp2 is dominated by highlands and shows a weak absorption with a minimum near 2.8 μm , characteristic of hydroxyl. Spectrum sp3 includes the south polar region and indicates both a broad absorption from about 2.8 to 3.1 μm , characteristic of trace adsorbed water, as well as a stronger 2.8- μm absorption, characteristic of hydroxyl. The water and hydroxyl absorptions are also seen in the sp2 and sp3 spectra with thermal emission. The colored dash-dot lines are continua that illustrate the 2.8- and 3- μm absorptions. For ease of comparison, the spectra were scaled by 0.8 (sp1), 0.565 (sp2), and 1.0 (sp3). (B) Continuum-removed spectra showing varying 3- μm absorptions. The green areas in Fig. 1F have spectral shapes like that in spectrum s2; the orange areas have an ~ 2.85 minimum like those in s5 to s7. (C) Spectrum s3 (top), from (B), is shown compared with laboratory spectra of minerals, a basalt, and a lunar soil. (D) VIMS lunar spectra s2 and s5, from (B), show broad absorption because of water with sharper absorptions attributed to hydroxyl. Spectra of minerals (11) show similar structure.



The olivine and anorthite are from (11), the basalt was measured for this study in (B), and the Apollo 16 soil is from the RELAB spectral library, www.planetary.brown.edu/relab. (D) VIMS lunar spectra s2 and s5, from (B), show broad absorption because of water with sharper absorptions attributed to hydroxyl. Spectra of minerals (11) show similar structure.

polar region and just north of Mare Crisium (Figs. 1E and 2B, spectra s6 and s7). Narrower absorptions, characteristic of hydroxyl fundamentals near 2.7 to 2.9 μm , are mapped in both the polar regions and in lunar highlands (Figs. 1F and 2B). The hydroxyl absorption mapped strongest in the polar regions and weaker but present at lower latitudes and along the lunar terminator (Fig. 1F). The lunar south polar region was tilted toward Cassini during the flyby, thus showing better coverage of that pole.

The host minerals for the water and hydroxyl are difficult to determine because the adsorbed water absorptions are not particularly unique and the 0.016- μm bandpass of the VIMS instrument was low. The position of the 3- μm absorption is consistent with ice as well as adsorbed water (Figs. 2, C and D, and 3), but ice is not stable in sunlight on the lunar surface. The water must be adsorbed or trapped in glass or in minerals. Adsorbed water has a wide range of wavelength positions and shapes that depend on the hydrogen bonding (16). The absorption minimum near 2.9 μm indicates that the water is strongly hydrogen bonded, which is also consistent with the harsh lunar environment, where only strongly bonded water might survive at the surface. Several minerals, including altered anorthite and pyroxenes, have hydroxyl fundamentals near 2.8 μm (15) and show spectral structure consistent with the lunar spectra.

Radiative transfer models (17) of typical lunar soil show that a water abundance of about 1000 ppm could produce a 2% absorption in VIMS spectra at 3 μm (Fig. 3). The strength of the absorption in the lunar spectrum sp3 in Fig. 2A is about 3%. A molecular mixture, where the water molecules are uniformly mixed in the lunar rocks or soils, has the highest sensitivity. For a typical grain size of 25 μm , models for a molecular mixture indicate that a 3% absorption would require about 10 ppm water if the reflectance were 40% (Fig. 3). For lower reflectances, higher water abundances are indicated. If the water was attached to some minerals and not others, and those minerals were in an intimate mixture, 3%

absorption would require 1000 ppm water at 40% reflectance. Laboratory dehydration experiments on basalt (SOM text) (fig. S4) show that a water content of 2500 ppm water at 18% reflectance yields a 9% absorption depth, so a 3% absorption would correspond to about 800 ppm, assuming a linear trend. The VIMS spectra are consistent with a water content of the sunlit lunar surface of 10 to 1000 ppm.

The 3- μm absorption detected by VIMS is confirmed by the Moon Mineralogy Mapper (M^3) on Chandrayaan-1 (18) and Deep Impact (DI) (19). DI confirms that the water absorption extends to low latitudes, but M^3 only shows absorption in the polar region because the limited spectral range makes low water amounts difficult to map. Both VIMS and DI data indicate stronger absorption near the lunar terminator, and Sunshine *et al.* (19) attribute this as evidence for movement of water with the diurnal cycle. However, viewing geometry might account for some or all of this apparent variability (SOM text and figs. S5 and S6).

LP (8–10) found relatively high concentrations of hydrogen at both lunar poles and smaller abundances at lower latitudes (Fig. 1F). The water detected by VIMS as well as M^3 and DI covers a larger area in the polar region than indicated by the LP hydrogen data. There is a correlation of the LP hydrogen data (Fig. 1G) and the VIMS absorptions (Fig. 1, E and F). Both VIMS and LP data indicate that the maria have low water content. The LP data represent a signal up to 1-m depth, whereas the VIMS data are sensitive to water and OH in the top millimeter or so of the surface. Water at the surface is more susceptible to destruction or escape than the buried hydrogen; thus, different patterns might be expected. The polar water seen in the VIMS data could be a thin surface effect from water migrating from low latitudes to the colder polar regions. Feldman *et al.* (8) argued against a surface deposit because it is not indicated by the fast neutron data. However, the neutron data are not sensitive to a low-abundance, very thin (mm) surface layer [see figure 3 in (8)], the depth probed by the VIMS data. This may indicate that the water and OH observed

in the VIMS data are not simply from a surface deposit in the polar regions but extend beneath the surface, and possibly have been mixed by impact gardening. At latitudes around the equator, VIMS detects some but not widespread water; however, hydroxyl is detected at all latitudes. The LP neutron data show high absorption near the equator (Fig. 1G) and may be indicating buried hydrogen that is too deep for VIMS to have detected.

About 10^{13} kg of water has been delivered to the lunar surface by comets over the past 2 billion years, or about 0.5 kg/m^2 (20). That amount distributed uniformly in the top millimeter of the surface would be about 50% abundance. Impact gardening would bury and mix that water in the top couple of meters, diluting the average abundance to about 500 ppm. The water that is detected by VIMS could be indicating the presence of that ancient water. Solar wind implanted protons could interact with oxygen-containing minerals and glasses in the lunar surface, creating H_2O and OH (21) species. Some of the signature reported here might originate from the solar wind protons. Regardless of its origin, water is found on the lunar surface in areas previously thought to have been depleted in volatiles.

References and Notes

1. K. Watson, B. C. Murray, H. Brown, *J. Geophys. Res.* **66**, 3033 (1961).
2. H. C. Urey, *The Planets: Their Origin and Development* (Yale Univ. Press, New Haven, CT, 1952).
3. P. Lucey *et al.*, *Rev. Mineral. Geochem.* **60**, 83 (2006).
4. R. M. Canup, *Annu. Rev. Astron. Astrophys.* **42**, 441 (2004).
5. P. C. Hess, E. M. Parmentier, *Earth Planet. Sci. Lett.* **134**, 501 (1995).
6. L. L. Hood, M. T. Zuber, in *Origin of the Earth and Moon*, R. M. Canup, K. Righter, Eds. (Univ. of Arizona Press, Tucson, AZ, 2000), pp. 397–409.
7. A. E. Saal *et al.*, *Nature* **454**, 192 (2008).
8. W. C. Feldman *et al.*, *Science* **281**, 1496 (1998).
9. W. C. Feldman *et al.*, *J. Geophys. Res.* **105**, 4175 (2000).
10. W. C. Feldman *et al.*, *J. Geophys. Res.* **106**, 23231 (2001).
11. R. H. Brown *et al.*, *Space Sci. Rev.* **115**, 111 (2004).
12. R. N. Clark, *Icarus* **40**, 94 (1979).
13. R. Clark, C. M. Pieters, Robert O. Green, and the M3 Science Team, *Lunar Planet. Sci.* **XL**, abstr. 2136 (2009).
14. S. K. Noble, C. M. Pieters, L. P. Keller, *Icarus* **192**, 629 (2007).
15. R. N. Clark *et al.*, U.S. Geological Survey, Data Series 231, <http://speclab.cr.usgs.gov/spectral-lib.html> (2007).
16. V. C. Farmer, Ed., *The Infra-Red Spectra of Minerals* (Mineralogical Society, London, 1974).
17. B. Hapke, *Theory of Reflectance and Emittance Spectroscopy* (Cambridge Univ. Press, New York, 1993).
18. C. M. Pieters *et al.*, *Science* **326**, 568 (2009); published online 24 September 2009 (10.1126/science.1178658).
19. J. M. Sunshine *et al.*, *Science* **326**, 565 (2009); published online 24 September 2009 (10.1126/science.1179788).
20. J. R. Arnold, *J. Geophys. Res.* **84**, 5659 (1979).
21. L. Starukhina, Y. Shkuratov, *Icarus* **147**, 585 (2000).
22. This research was funded by NASA Cassini VIMS under contract to the U.S. Geological Survey; R.C. is a VIMS team member.

Supporting Online Material

www.sciencemag.org/cgi/content/full/1178105/DC1
Materials and Methods
SOM Text
Figs. S1 to S6
References

22 June 2009; accepted 15 September 2009
Published online 24 September 2009;
10.1126/science.1178105
Include this information when citing this paper.

Fig. 3. Radiative transfer models of water and hydroxyl-bearing minerals in different conditions and amounts on a model of Apollo 16 soil (containing no water or hydroxyl absorptions). Different scattering conditions and water abundances change the strength of the 3- μm water absorption.

